150. Intramolecular Dynamics of Tetranuclear Iridium Carbonyl Cluster Compounds

Part IV[1])

Derivatives with Monodentate Ligands and Edge-Bridging Bidentate Ligands

by **Andrès Strawczynski**[2]), **Gianfranco Suardi**[2]), **Renzo Ros**[3]), and **Raymond Roulet***

Institut de Chimie Minérale et Analytique de l'Université, 3, place du Château, CH–1005 Lausanne

(20.IV.93)

The fluxionality of $[Ir_4(CO)_8(\mu_2\text{-}CO)_3L]$ (L = Br^-, I^-, SCN^-, NO_2^-, $P(4\text{-}ClC_6H_4)_3$, PPh_3, $P(4\text{-}MeOC_6H_4)_3$, $P(4\text{-}Me_2NC_6H_4)_3$), as studied by 2D-^{13}C-NMR in solution, is due to two successive scrambling processes: the merry-go-round of six basal CO's and CO bridging to alternative faces of the Ir_4 tetrahedron. The basicity of the ligand L has no significant effect on the activation parameters. The scrambling process of lowest activation energy in $[Ir_4(CO)_7(\mu_2\text{-}CO)_3(PMePh_2)_2]$ correspond to the two possible synchronous CO bridging about a unique face of the metal tetrahedron swapping the relative axial and radial positions of the ligands L. The disubstituted clusters $[Ir_4(CO)_{10}(\mu_2\text{-}L\text{–}L)]$ with one edge-bridging ligand have a ground-state geometry with three edge-bridging CO's (L–L = bis(diphenylphosphino)methane, bis(diphenylarsino)methane, bis(diphenylphosphino)propane) or with all terminal CO's (L–L = $CH_3SCH_2SCH_3$). In all cases, the fluxional process of lowest activation energy in the merry-go-round of six CO's about a unique triangular face. For the P and As donor ligands, this process is followed by the rotation of terminal CO's bonded to two Ir-atoms residing on the mirror plane of the unbridged intermediate.

Introduction. – The substituted derivatives of $[Ir_4(CO)_{12}]$ generally have CO ligands that either bridge two Ir-atoms or are terminal. The three bridging CO's define the basal face containing three Ir-atoms of the metal tetrahedron. Terminal CO's are either apical if located on the fourth Ir-atom, radial when located more or less in the basal plane, or axial if approximately perpendicular to the basal plane. The fluxional behaviours of seven monosubstituted $[Ir_4(CO)_{11}L]$ clusters have been examined to date (L = PEt_3 [2] [3], $PMePh_2$ [4], PH_2Ph, $PHPh_2$ [5], Br^- [6], SO_2 [7], *t*-BuNC [8] [9]). The PEt_3 and Br^- complexes have the same ground-state geometry with three bridging CO's and one axial L ligand, and behave similarly. The μ_2-SO_2 complex has two edge-bridging CO's, and the CO site exchanges are due to a change in basal face. The *t*-BuNC complex has all terminal ligands, [10] and its fluxional behaviour, recently reassessed [9], is due to two successive merry-go-rounds of CO's causing *Cotton*-like scrambling and a CO rotation about one metal centre. We now report a 2D-NMR study of eight additional, isostructural $[Ir_4(CO)_{11}L]$ clusters to ascertain the generality of the observed processes and the influence of the basicity of the L ligand on the activation parameters.

[1]) Part III: [1].

[2]) In part from the doctoral dissertations of *A. S.* and *G. S.*, University of Lausanne.

[3]) Permanent address: Istituto di Chimica Industriale dell'Università, Via Marzolo 9, I–35131 Padova.

The complex pathways for CO scrambling in disubstituted $[Ir_4(CO)_{10}L_2]$ complexes with monodentate L ligands have not yet been elucidated. We report here on the lowest-activation-energy scrambling processes in $[Ir_4(CO)_{10}(PMePh_2)_2]$. The fluxional behaviour of two disubstituted complexes with one chelating ligand, $[Ir_4(CO)_{10}$(cycloocta-1,5-diene)] and $[Ir_4(CO)_{10}$(diarsine)] has been examined in a previous article of this series [11]. We report now on the intramolecular dynamics of four other disubstituted Ir_4 complexes with one edge-bridging, bidentate ligand.

Monosubstituted Complexes. – The $[Ir_4(CO)_{11}L]$ complexes enriched to *ca.* 30% in ^{13}C (L = Br^-, **1**; I^-, **2**; NCS^-, **3** [12]; NO_2^-, **4**; NCO^-, **5** [13]; P(4-$ClC_6H_4)_3$, **6**; PPh_3, **7** [14–16]; P(4-$(MeO)C_6H_4)_3$, **8**; P(4-$(Me_2N)C_6H_4)_3$, **9**) have been obtained in excellent yields by CO displacement from $[Ir_4(CO)_{12}]$ with $[NEt_4]Br$, $[NEt_4]I$, or $(PPN)N_3$ for **1**, **2**, and **5**, respectively, or by the reaction of the NEt_4^+ salt of **2** with AgSCN, $AgNO_2$, or PAr_3 for **3**, **4**, and **6–9**, respectively.

The ^{13}C-NMR spectrum of **5** in (D_8)THF/$CHFCl_2$ 1:1 presents a single CO resonance down to 135 K. Its unexpectedly high fluxionality with respect to the NMR time scale prevented its study in solution. The ^{13}C-NMR spectra of **2–4** and **6–9** are blocked at *ca.* 160 K. Seven resonances are observed with relative intensities 2:1:1:2:2:2:1 (see *Experimental*). Their assignment follows the general observation that in the ^{13}C- and ^{13}P-NMR spectra of Ir_4 cluster compounds, the δ's of the ligands decrease in the positional sequence bridging > radial > axial ≈ apical [16]. The two resonances with highest δ's are found in the region characteristic of bridging CO's. The ^{31}P $\Delta\delta$'s of **6–9** are in accordance with PAr_3 ligands in axial positions. Only one isomer is observed in solution, even though two isomers of **3** have been characterised in the solid state [17] [18]. Therefore, all complexes clearly have the same ground-state geometry in solution as that reported for **1** [6], whose crystal structure has been determined [19] (*Scheme 1*, left). The lettering follows that

Scheme 1

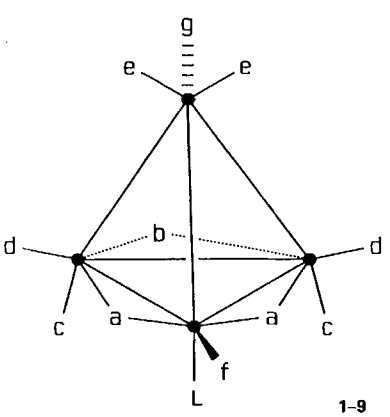

1–9

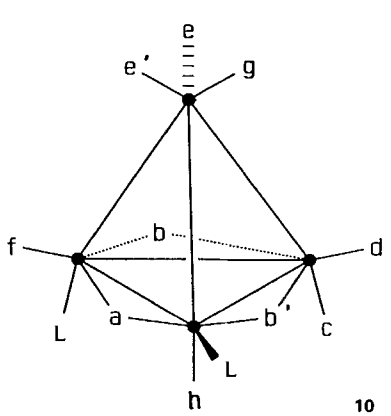

10

chosen earlier for **1**. CO Groups *c* and *e* show a pseudo-*trans*-$^{13}C,^{13}C$ coupling in the COSY spectra and are indistinguishable, but fortunately a more precise assignment is of no importance for the discussion of the fluxionality of these complexes.

The dynamic connectivities of the signals were established by 2D-NOESY-^{13}C-NMR at two different temperatures. An example corresponding to **9** is given in *Fig. 1*. At 205 K,

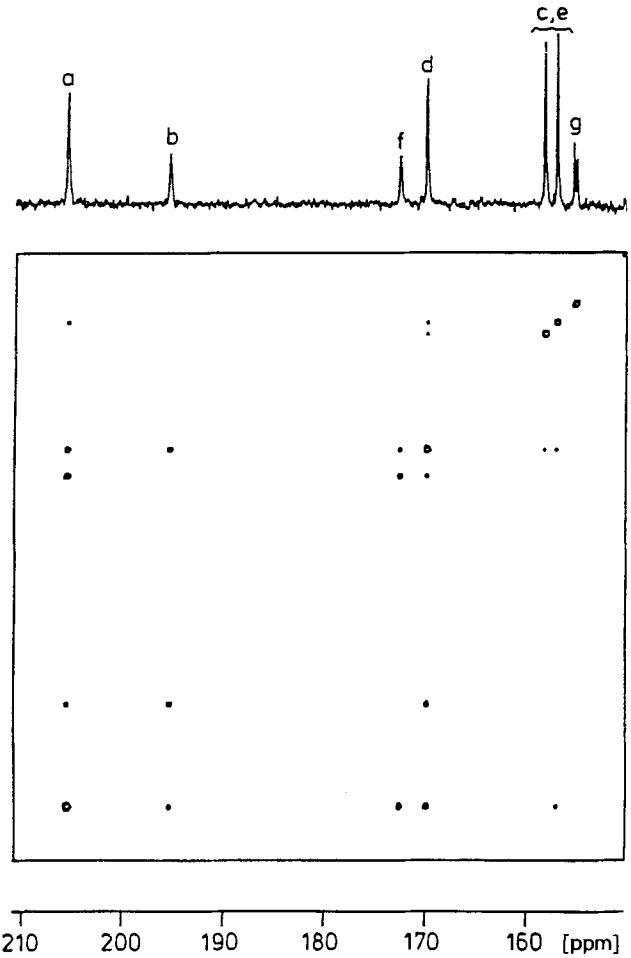

Fig. 1. *2D-NOESY ^{13}C-NMR Spectra of* **9** *in CD_2Cl_2 at 210 K* (mixing time: 100 ms)

the only site exchange present is *a-d-b-f*. Thus, the first fluxional process is the merry-go-round of the six basal CO's. At 210 K, a second process adds significantly to the first one, and second-order peaks could be identified using the D2DNMR computer program [20]. The second process corresponds to a site exchange *d-c-e* keeping CO *g* in pseudo-*trans*-position relative to L. Since apical-basal site exchange is observed, the second process involves CO ligands bridging to alternative faces of the Ir_4 tetrahedron. The exchange matrix previously used for **1** [6] is, thus, valid for **2–4** and **6–9** and was used to evaluate the rate constant *k* of the two processes from line-shape analysis [21] of the variable temperature ^{13}C-NMR spectra (example in *Fig. 2*).

The activation parameters were calculated from the graphs $\ln(k/T)$ *vs.* $1/T$ and are collected in the *Table*.

The four PAr_3 ligands have the same cone angle (145°) and a basicity increasing along the sequence *p*-ClC_6H_4 < Ph < *p*-$(MeO)C_6H_4$ < *p*-$(Me_2N)C_6H_4$ in accordance with their

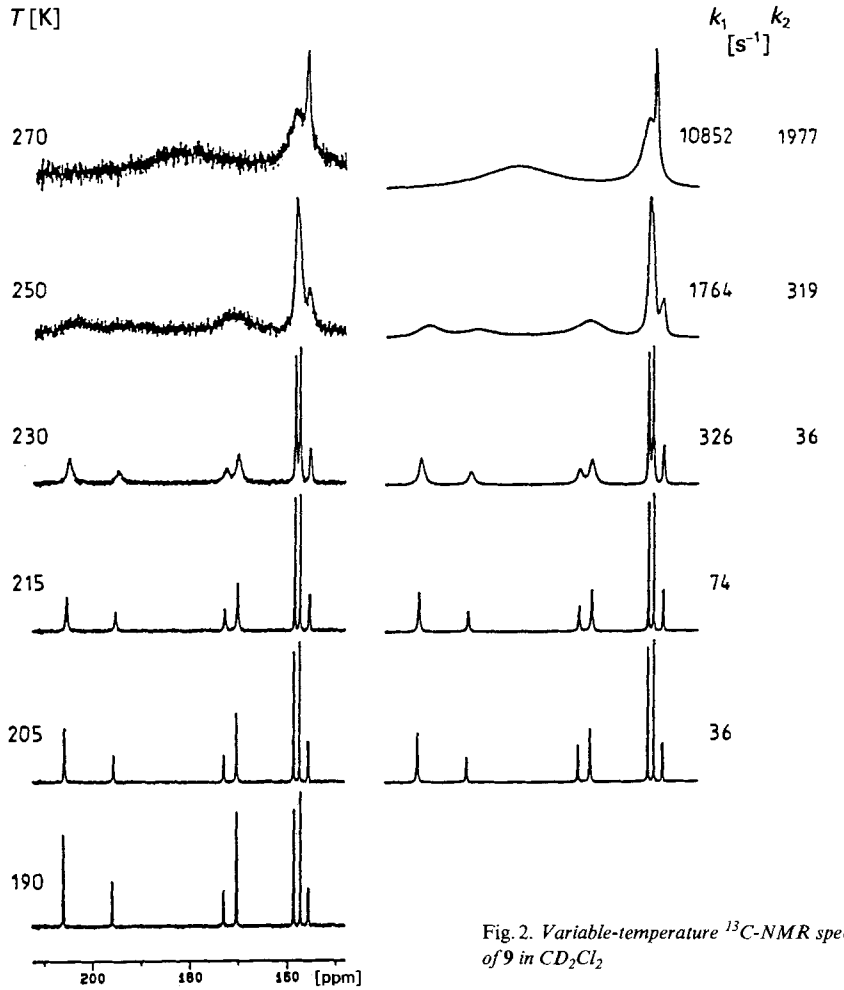

Fig. 2. *Variable-temperature ^{13}C-NMR spectra of* **9** *in CD_2Cl_2*

Table. *Activation Parameters of the Fluxional Process in $[Ir_4(CO)_{11}L]$ at 298 K.* $\Delta H^{\ddagger}$ and $\Delta G^{\ddagger}$ in kJ mol^{-1}, $\Delta S^{\ddagger}$ in J mol^{-1}K^{-1}, 2 σ in parentheses.

	L[a])	Merry-go-round			Change of face
		$\Delta G^{\ddagger}$	$\Delta H^{\ddagger}$	$\Delta S^{\ddagger}$	$\Delta G^{\ddagger}$
1	Br^-	37.0 (0.6)	33 (1)	–13 (6)	35 (4)
2	I^-	36.8 (0.4)	34 (2)	–9 (2)	38.6 (0.4)
6	$P(4\text{-}ClC_6H_4)_3$	46.6 (0.5)	36.7 (1.5)	–33 (7)	46.7 (0.9)
7	PPh_3	45.6 (0.4)	40.0 (0.4)	–19 (3)	46.3 (0.5)
8	$P(4\text{-}(MeO)C_6H_4)_3$	46.3 (0.4)	40.3 (0.4)	–20 (2)	47.0 (0.4)
9	$P(4\text{-}(Me_2N)C_6H_4)_3$	45.8 (0.6)	41.1 (1.6)	–16 (7)	48.6 (0.4)

[a]) For SCN^- and NO_2^-, $\Delta G^{\ddagger} = 33 \pm 2$ and 40.7 ± 0.9 kJ mol^{-1}, respectively, for the merry-go-round. For NO_2^-, $\Delta G^{\ddagger} = 44 \pm 2$ kJ mol^{-1} for the change of face. Lack of sufficient data at higher temperature prevented the evaluation of the corresponding $\Delta G^{\ddagger}$ for SCN^-.

Tolman X parameters (16.8, 13.2, 10.5, and 5.3, respectively [22]). The comparison of the data for **1–2** and for **6–9** shows that the basicity of the ligand L has no significant effect on the activation parameters of the fluxional processes. We have recently shown that the intermediate of the merry-go-round process is the unbridged isomer, and that its transition state should have a geometry with three semi-bridging CO's by comparing the activation volume $\Delta V^{\ddagger}$ and the reaction volume of the isomerisation of $[Ir_4(CO)_6(\mu_2\text{-}CO_3)(1,3,5\text{-trithiane})]$ [23]. All $\Delta S^{\ddagger}$'s in the *Table* are negative and may be in accordance with semi-bridging CO's having more degrees of freedom than edge-bridging CO's. The $\Delta V^{\ddagger}$ of a change of face is unknown, therefore, only the $\Delta G^{\ddagger}$'s are reported for the second process.

Complex $[Ir_4(CO)_{10}(PMePh_2)_2]$ (10). – The direct reaction of $[Ir_4(CO)_{12}]$ with $PMePh_2$ gives a mixture of four complexes [4]. The formation of tri- and tetrasubstituted complexes was avoided by reacting **1** with 1.7 mol-equiv. $PMePh_2$ at 0° in CH_2Cl_2. Chromatography of the products gave $[Ir_4(CO)_{11}(PMePh_2)]$ (27%) and **10** (55%). The ^{31}P-NMR spectrum of **10** in (D_8)toluene at 240 K presents two resonances at −28.8 and −6.7 ppm relative to external H_3PO_4 85% which correspond to P-atoms in radial and axial positions ($\Delta\delta = -1.0$ and +21.1 ppm, respectively). Upon raising the temperature, the signals coalesce at *ca.* 330 K. Simulation of the experimental spectra [21] followed by an *Eyring* regression of $\ln(k/T)$ *vs.* $1/T$ gave a free enthalpy of activation of 56.7 ± 0.4 kJ mol^{-1} (at 298 K) for the two sites exchange.

In the ^{13}C-NMR spectrum of a ^{13}C-enriched sample of **10** in CD_2Cl_2, all exchange processes are blocked at *ca.* 225 K: ten resonances are observed at δ 217.5, *a*; 206.0, 204.5, *b* and *b'*; 176.1 (*dd*, *J*(C,P) = 9 and 8 Hz), *f*; 173.6 (*d*, *J* = 15 Hz), *d*; 161.9, 160.9, *c* and *e*; 160.6 (*d*, *J* = 25 Hz), *g*; 159.7 (*d*, *J* = 6 Hz), *h*; 157.2 ppm, *e'* (see *Scheme 1*, right). The first three signals are unambiguously due to edge-bridging CO's, but *b* and *b'* cannot be individually assigned. The signals at 161.9 and 160.9 present at ^{13}C,^{13}C coupling in the COSY spectrum. They correspond to CO's in pseudo-*trans*-positions (*c* and *e*) but cannot be further distinguished. Upon raising the temperature, exchanges between bridging, apical, radial, and axial CO's are observed. Therefore, the CO-scrambling processes responsible for the observed P-atoms site exchange are too complex to be simulated, and only the processes with lowest activation energy could be identified.

The dynamic connectivities were deduced from a 2D-NOESY ^{13}C-NMR spectrum at 250 K (*Fig. 3*). Radial-apical exchanges are observed which must be due to change(s) of the basal face of the Ir_4 tetrahedron. A change of face may take place through an unbridged intermediate (*Scheme 2*, mechanism *III*), as reported by *Stutz* and *Shapley* for $[Ir_4(CO)_{11}(PMePh_2)]$ [4] and by *Mann et al.* for $[Ir_4(CO)_{11}(PH_{3-n}Ph_n)]$ (n = 1 or 2) [5]. It may also proceed synchronously (without passing through an unbridged intermediate) as observed for **1** [5] and for **2–4**, **6–9** (see above), and for $[Ir_4(CO)_{11}(\mu_2\text{-}SO_2)]$ [7]. In the present case, CO *a* does not exchange with other CO's in the lowest activation energy process(es). This excludes any merry-go-round of basal CO's as well as a change of face going through an unbridged intermediate, since an *a–h* exchange is not observed (mechanism *III*). A projection on the F_2 axis of the row containing the first-order peak at 206.0 ppm (*b* or *b'*) showed that it exchanges with the peaks of 204.5 and 160.6 ppm. Therefore, two processes are operating about simultaneously. As CO *a* bridges the Ir_1–Ir_3 edge, these processes must correspond to the two possible synchronous CO bridging about the

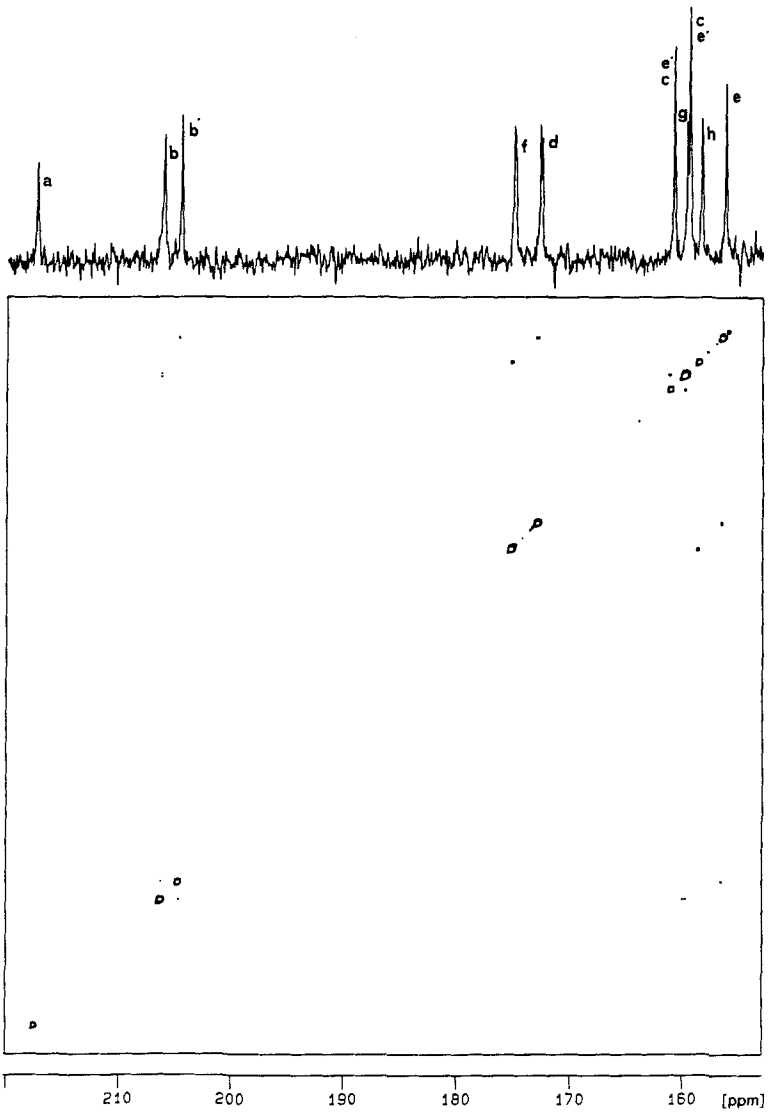

Fig. 3. *2D-NOESY ^{13}C-NMR Spectra of* **10** *in CD_2Cl_2 at 250 K* (mixing time: 100 ms)

Ir_1–Ir_3–Ir_4 face (*Scheme 2*, mechanisms *I* and *II*). The signal at 160.6 ppm is a *doublet* and can unambiguously be assigned to CO *g* which is the only apical CO located in a pseudo-*trans*-position to a P-atom. As CO *g* cannot bridge the Ir_1–Ir_4 edge, a *b'-g* exchange cannot occur in a single step, and the signal at 206.0 ppm can be assigned to CO *b*. The observed exchange *b-g* and *b-b'* correspond to mechanisms *I* and *II*, respectively. The signal at 204.5 ppm being now attributed to CO *b'*, the observed *b'-e* and *d-g* exchanges belong to mechanism *I* and the *d-e* exchange to mechanism *II*. The mutual

Scheme 2

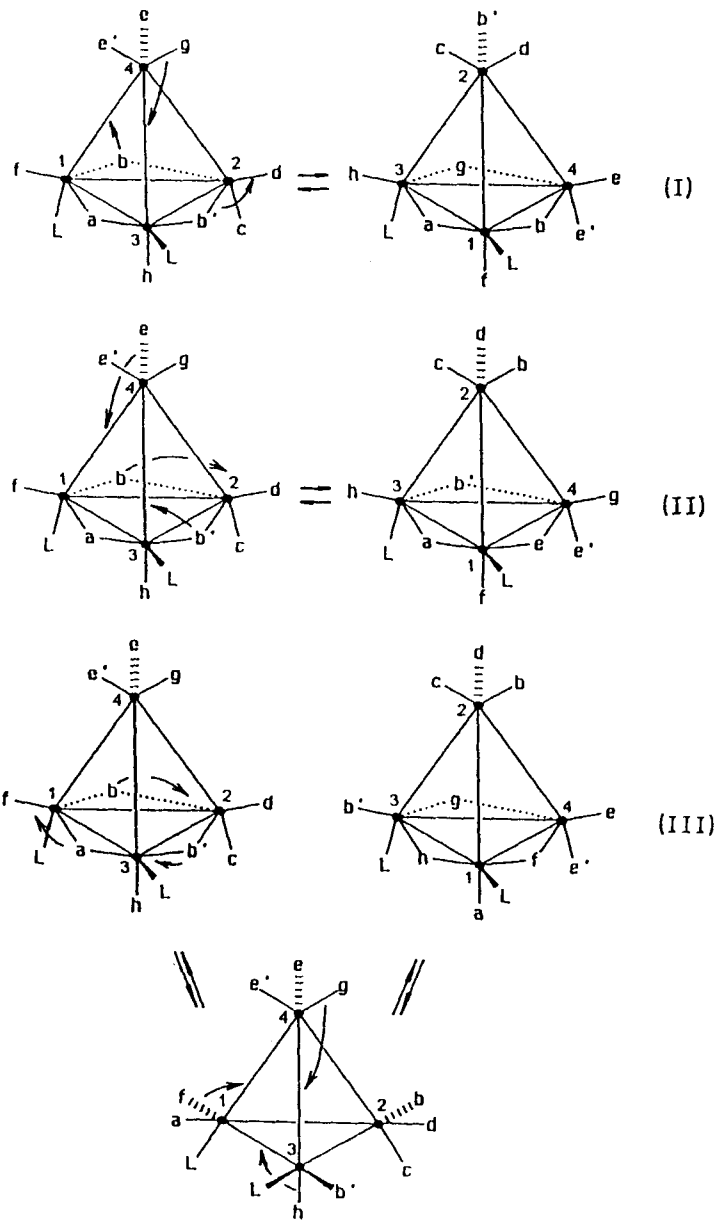

exchanges *f*-*h* and *c'*-*e* are common to both mechanisms. Upon raising the temperature above 250 K, the NOESY spectra recorded with mixing times up to 120 ms show that CO *a* starts to exchange with *h*, but were too complicated to be interpreted.

A search for other disubstituted complexes with PR_3, $P(OR)_3$, or RNC ligands having the same ground-state geometry as that of **10** was unsuccessful, either because several

isomers were present in solution, or the time scale of the fluxional process was unfit for an NMR study. The disubstituted complex $[Ir_4(CO)_{10}(\eta_1\text{-dppb})_2]$ (dppb = bis(diphenylphosphino)butane) could be isolated from the reaction of $[Ir_4(CO)_{10}$(cycloocta-1,5-diene)] and dppb in CH_2Cl_2 at −20° [24]. Its ^{31}P- and ^{13}C-NMR spectra (see *Exper. Part*) show that this complex has the same geometry as that of **10**, each dppb ligand being coordinated through one P-atom. However, CO displacement by the free diphenylphosphino groups slowly takes place above 272 K giving $[Ir_4(CO)_8(\mu_2\text{-dppb})_2]$ [16] [25] and other unidentified products.

Disubstituted Complexes with One Edge-Bridging Bidentate Ligand. – The complexes $[Ir_4(CO)_{10}(\mu_2\text{-dppp})]$ (**11**, dppp = bis(diphenylphosphino)propane) and $[Ir_4(CO)_{10}(\mu_2\text{-dppm})]$ (**12**; dppm = bis(diphenylphosphino)methane) were first prepared by *Ros et al.* [16] from **1** and the corresponding diphosphine (*Scheme 3*). Their crystal structures were

Scheme 3

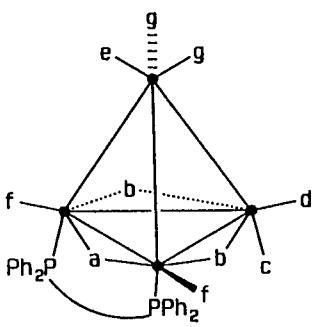

11, 12

not determined, but their spectral characteristics are quite similar to those of $[Ir_4(CO)_{10}(\mu_2\text{-}Me_2PCH_2CH_2PMe_2)]$ which has been characterised by X-ray diffraction [16]. The latter complex presents three edge-bridging CO's and two axially located P-atoms with respect to the basal face. The ^{31}P-NMR spectrum of **11** presents one resonance with a coordination chemical shift of −3.1 ppm which is characteristic of a diaxial substitution.

In the ^{13}C-NMR spectrum of a ^{13}C-enriched sample of **11** in (D_8)toluene, all exchange processes are stopped at *ca.* 240 K. At this temperature seven CO resonances are observed at δ (relative to TMS) 222.1, *a*; 200.8, *b*; 174.6, *f*; 172.5, *d*; 164.7, 160.0 *c* and *e*; 157.1 ppm, *g*, with relative intensities 1:2:2:1:1:1:2, respectively. The signal at 157.1 ppm is a *doublet* with J(C,P) = 27.4 Hz. Since the largest coupling in Ir_4 clusters occurs between nuclei in pseudo-*trans*-position [16], the resonance at 157.1 ppm can confidently be assigned to CO *g*. The assignment of CO's *c* and *e*, however, is ambiguous, and this will have to be taken into account in the discussion of the fluxional processes.

The diaxial geometry of **12** cannot be inferred with certainty from the ^{31}P-NMR spectra (one signal with $\Delta\delta = -29.5$ ppm [16]), but is deduced from the exclusion of other alternative geometries. The ^{13}C-NMR spectrum of ^{13}C-enriched sample of **12** in CD_2Cl_2 at 185 K is quite similar to that of **11**. At this temperature, all exchange processes are stopped, and seven CO resonances are observed at δ 221.7, *a*; 205.6, *b*; 178.5, *f*; 171.0, *d*;

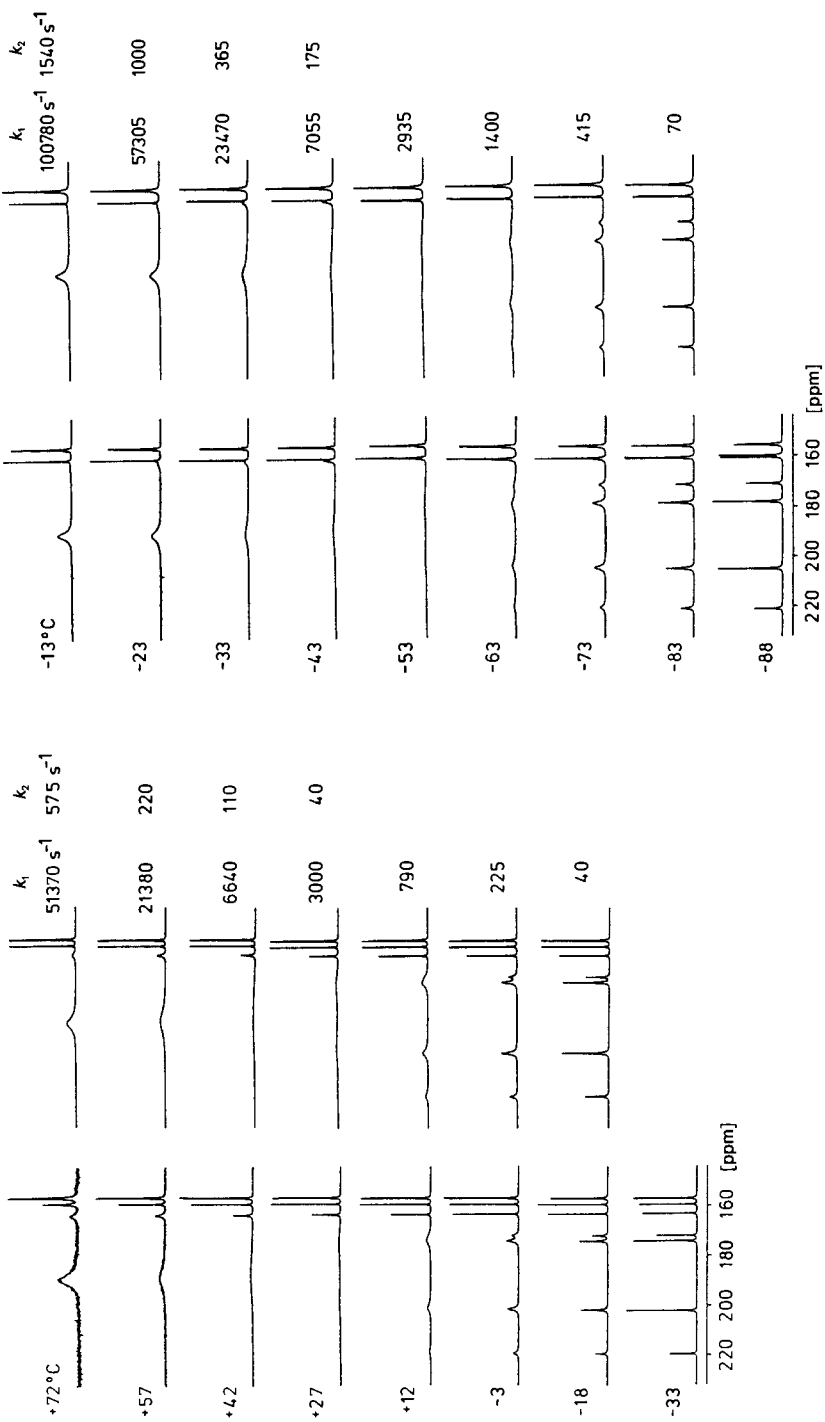

Fig. 4. *Variable-temperature ^{13}C-NMR spectra of* **11** (left) *and* **12** (right) *in (D_8)toluene and CD_2Cl_2, respectively*

161.3, 160.3, *c* and *e*; 156.3 ppm, *g*, with relative intensities 1:2:2:1:1:1:2, respectively. Its ^{1}H-NMR spectrum in $CDCl_3$ presents two CH_2 signals at 5.30 and 2.92 ppm [16]. The possible geometries with a chelating dppm, or with an edge-bridging dppm in axial-radial or axial-apical positions have to be discarded on the basis of the NMR spectra. The alternative geometry with a diradially bridging dppm is eliminated on the grounds of the number of ^{13}C-NMR signals appearing in the region characteristic of radial CO's (two signals with relative intensities 2:1 as for **11**). Molecular models show that a diradial substitution may occur only when the aliphatic chain of the diphosphine contains at least

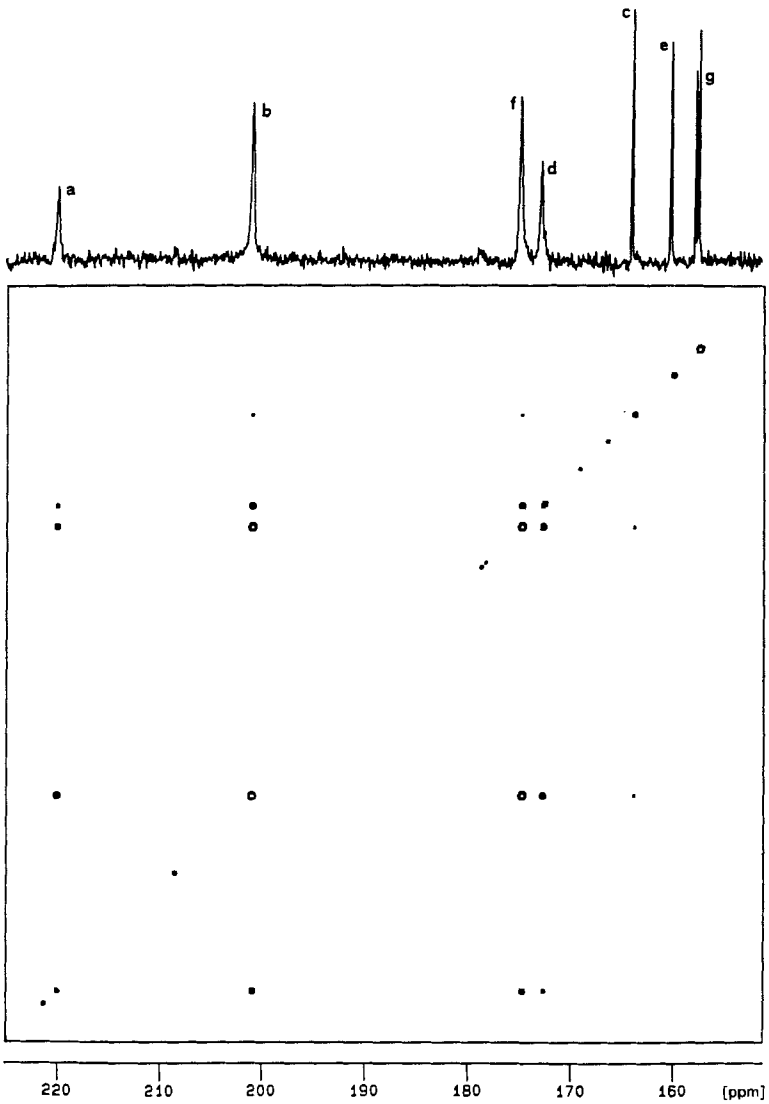

Fig. 5. *2D-NOESY ^{13}C-NMR spectrum of* **11** *in CD_2Cl_2 at 250 K* (mixing time: 400 ms)

four C-atoms. Furthermore, the crystal structure of $[M_4(CO)_8(\mu_2\text{-dppm})_2]$ (M = Rh [26], Ir [27]) shows that the dppm ligand that is bonded to the basal metal atoms occupies two axial positions. Therefore, a diaxial geometry can confidently be proposed for **11** and **12**. The analogous $\delta(^{31}P)$ of dppm in **12** is probably due to different dihedral P–Ir–Ir–P angles and P–P distances, which also seem to be responsible for the multiplicity of the ^{13}C-NMR signal at 156.9 ppm, assigned to CO *g*. At 220 K, this signal appears as a *quintet* which was successfully simulated as an A_2XX' spin system with $J(C,P) = 32$ and $J(P,P) = 39$ Hz (the contribution of $^{13}C,^{13}C$ couplings are negligible). The value of $J(C,P)$ is in agreement with a pseudo-*trans*-arrangement of each CO *g* and a P-atom.

The variable-temperature ^{13}C-NMR spectra of **11** and **12** (*Fig. 4*) indicate that two similar CO-exchange processes occur in both complexes. The lowest-activation-energy process involves CO's *a-f-b-d* and is clearly the merry-go-round of basal CO's. Then, the signals at 164.7 ppm for **11**, and 161.3 ppm for **12**, start to broaden. A 2D-NOESY ^{13}C-NMR spectrum of **11** in CD_2Cl_2 at 255 K (*Fig. 5*) confirms the dynamic connectivity *a-f-b-d*, and the projection on the F_2 axis of the row corresponding to the signal at 164.7 ppm shows that it exchanges preferentially with that of CO's *b*. The signal at 164.7 ppm can be assigned to CO *c* and not to *e* on the following grounds: if the second process

Scheme 4

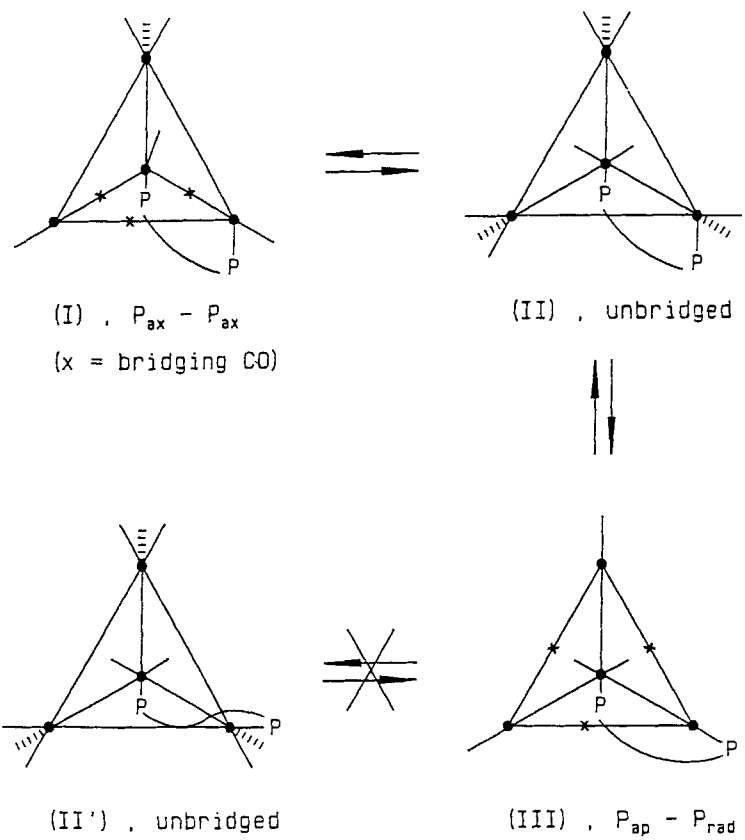

involves CO *e*, an apical-basal exchange of CO's must take place. This is brought about by successive edge-bridging of CO's to two alternative faces of the tetrahedral metal core (the second change of face is necessary to restore the two P-atoms back to their original configuration). The double change of face either proceeds through unbridged intermediates or is synchronous. In the first case, since a configuration with two radial P-atoms is not allowed, the successive steps would have to pass through an unbridged intermediate *II'* with a configuration which must be excluded on steric grounds (*Scheme 4*).

The second alternative is two changes of basal face which do not pass through unbridged intermediates. This would result in an exchange between CO's *g* and *b*, which is not observed for **11** and **12**. Therefore, CO *e* cannot be involved in the CO exchange without incorporating *g* in the process. Thus, the signal at 163.0 ppm for **11** was assigned to CO *c*, and the second fluxional process in both complexes corresponds to an exchange *b-d-c*.

The CO exchange processes are more rapid for **12** than for **11**. A third site-exchange process is observed for the dppm complex on further raising the temperature (*Fig. 6*),

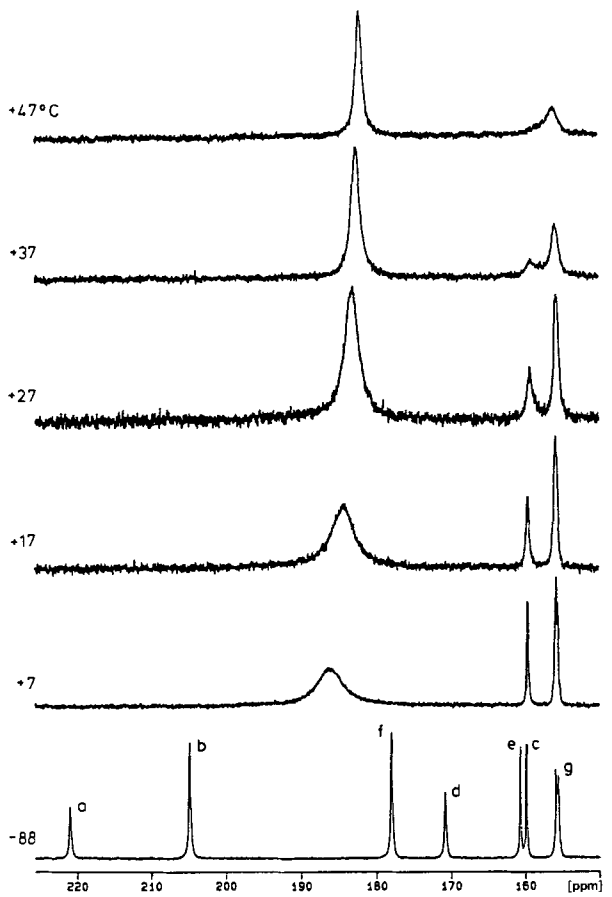

Fig. 6. *^{13}C-NMR Spectra of* **12** *in (D_8)toluene at and above 280 K*

which is clearly a two site exchange due to the rotation of apical CO's about a local C_3 axis.

If the first and third processes are clearly the merry-go-round of basal CO's and the rotation of apical CO's, respectively, the second process involving the exchange *c*-*b* can be explained by two mechanisms (*Scheme 5*). *i*) The axial CO *c* is incorporated in the merry-go-round ($I \leftrightarrow II$): A matrix based on the exchange $a \rightarrow f \rightarrow b \rightarrow c \rightarrow b \rightarrow f \rightarrow a$ simulates fairly well the observed spectra. However, such a mechanism has never been observed for other Ir_4 cluster compounds or any other cluster compound. *ii*) The rotation of CO's bonded to the basal Ir-atom residing on the mirror plane of the molecule. The matrix based on the exchange $c \rightarrow b \rightarrow d \rightarrow c$ was used for the successful simulations reported in *Fig. 4*. The unbridged intermediate *III* may effectively be formed during the first process (the merry-go-round), and could also be responsible for the third process (the rotation of apical CO's).

Scheme 5

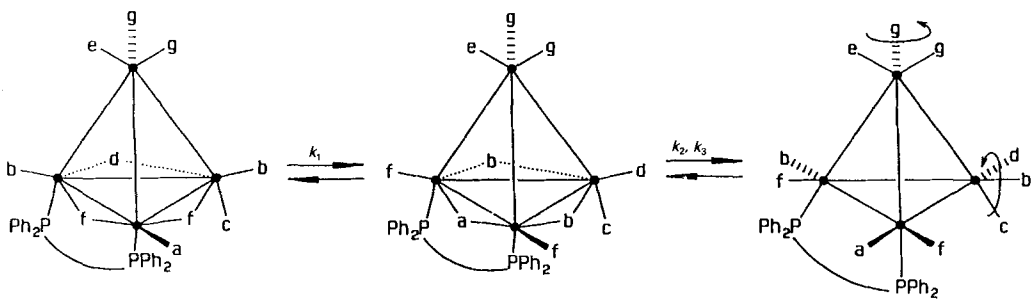

The rate constants k_1, k_2, and k_3 of the three processes were evaluated from line-shape analysis [21] of the variable-temperature ^{13}C-NMR spectra using the following *Kubo-Sack* matrix elements [28]: *1*) For the first two processes: $(a,a) = (d,d) = (f,f) = -k_1$; $(b,b) = -k_1 - k_2/2$; $(d,d) = -k_1 - k_2$; $(c,c) = -k_2$; $(a,f) = (d,b) = k_1$; $(f,a) = (f,b) = (b,f) = k_1/2$; $(b,d) = k_2/2$; $(d,c) = (c,b) = k_2$. *2*) For the third process: $(e,e) = -k_3$; $(g,g) = -k_3/2$; $(e,g) = k_3$; $(g,e) = k_3/2$.

The activation free enthalpies calculated from the graphs $\ln(k/T)$ *vs.* $1/T$ are: $\Delta G_1^{\ddagger} = 53.9 \pm 0.1$ for **11**, 38.0 ± 0.5 kJ mol^{-1} for **12**; $\Delta G_2^{\ddagger} = 64.2 \pm 0.3$ for **11**, 49.0 ± 1.1 kJ mol^{-1} for **12**; $\Delta G_3^{\ddagger} > 80$, for **11**, 60.7 ± 0.2 kJ mol^{-1} for **12**.

The merry-go-round (as well as the two other site exchange processes) are faster in **12** than in **11**. This is probably due to a greater cyclic tension in the $Ir_2(\mu_2$-dppm) fragment (a five-membered ring) than in $Ir_2(\mu_2$-dppp) (a six-membered ring). *Braga* and *Grepioni* have found from a compilation of crystallographic data that the Ir_4 core of a cluster having all terminal ligands is smaller than the core of a cluster with three edge-bridging CO's [29]. Therefore, cyclic tension should decrease on going from a CO-bridged geometry to an unbridged geometry. The unbridged intermediate (or transition state) or the merry-go-round in **12** should thus be more stabilised than the corresponding one in **11**.

The disubstituted cluster $[Ir_4(CO)_{10}(\mu_2$-dpam)] (**13**; dpam = bis(diphenylarsino)-methane) was obtained from the reaction of **2** with 1 mol-equiv. of dpam and of Ag[BF_4] in THF. Its IR spectrum in cyclohexane shows two bands at 1841 and 1798 cm^{-1} due to

edge-bridging CO's. The ^{13}C-NMR spectrum of a sample of **13** enriched to *ca.* 30%. ^{13}C in (D_8)THF is blocked at 160 K and presents seven resonances at δ 224.4, *a*; 208.5, *b*; 178.7, *f*; 174.9, *d*; 161.0, 159.4 (*c* and *e*); 157.2 ppm *g*, with the relative intensities 1:2:2:1:1:1:2, suggesting the same ground-state structure as that of **11**. The 2D-NOESY (mixing time: 400 ms) and the variable-temperature ^{13}C-NMR spectra (160–250 K) in (D_8)THF are quite similar to those of **11** and were simulated using the exchange matrix given above. The calculated $\Delta G^{\ddagger}$'s at 298 K are 32.3 ± 0.5 kJ mol^{-1} for the merry-go-round and 42.7 ± 3.2 kJ mol^{-1} for the second process.

The disubstituted cluster [$Ir_4(CO)_{10}(\mu_2$-$CH_3SCH_2SCH_3)$] (**14**) was obtained from the reaction of **2** with 1 mol-equiv. of bis(methylthio)methane and of Ag[BF_4] in CH_2Cl_2 at −15°. Its IR spectrum in nujol indicates that all CO's are terminal. However, in CH_2Cl_2, two very weak absorptions are present at 1829 and 1787 cm^{-1} and suggest the presence of the CO-bridged, minor isomer. In contrast to [$Ir_4(CO)_9$(1,3,5-trithiane)], the IR spectra of **14** in CH_2Cl_2 and THF are temperature-independent (183–298 K), and an isomerisation process between the CO-bridged and the unbridged isomers is unlikely. The ^{13}C-NMR spectrum of **14** in CD_2Cl_2 is blocked at 168 K and presents six resonances at 168.0, *a*; 164.6, *b*; 163.8, *c*; 158.2, *d*; 156.8, *g*; 154.1 ppm, *e*, with the relative intensities 2:2:1:2:2:1. The assignment was based on the observed ^{13}C,^{13}C couplings in a 2D-COSY spectrum. No resonances were found in the region characteristic of bridged CO's. Therefore, the proposed ground state structure of **14** is that of the unbridged isomer (*Scheme 6*).

Scheme 6

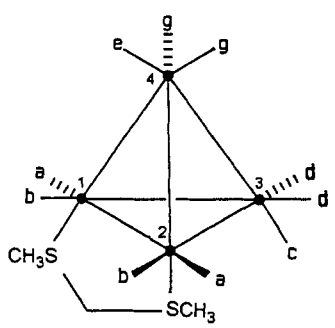

A 2D-NOESY ^{13}C-NMR spectrum of **14** in CD_2Cl_2 at 186 K (mixing time: 20 ms) presents the dynamic connectivities *a*-(*b*,*d*), *b*-*a*, and *d*-*a*. Therefore, the exchange process of lowest activation energy is the merry-go-round of six CO's around the Ir_1–Ir_2–Ir_3 face. The variable-temperature ^{13}C-NMR spectra (168–248 K) shows the coalescence of the *a*-*b*-*d* signals and no change in signal *g*. However, a second, unidentified process is present and becomes significant above 188 K, since the resonances of CO's *c* and *e* start to broaden, and no successful simulation could be found.

In conclusion, we propose that the scrambling process of lowest activation energy in [$Ir_4(CO)_8(\mu_2$-$CO)_3$L] and [$Ir_4(CO)_{10}(\mu_2$-L–L)] cluster compounds is the merry-go-round of six CO's around the triangular face of the metal tetrahedron which is more or less perpendicular to the Ir–L bond(s). In the monosubstituted complexes, the merry-go-round process, whose activation energy is independent of the basicity of the ligand L, is

followed by two consecutive changes of face causing apical-basal CO scrambling. In the disubstituted complexes having an edge-bridging bidentate ligand with P- or As-donor atoms, the merry-go-round is followed by the rotation of terminal CO's bonded to the two Ir-atoms residing on the mirror plane of the unbridged intermediate. In $[Ir_4(CO)_7(\mu_2\text{-}CO)_3(PMePh_2)_2]$, where the radial position of one non-CO ligand forbids the merry-go-round of basal CO's, the scrambling processes with lowest activation energy correspond to the two possible, synchronous CO bridgings about the face containing the apical and the two substituted Ir-atoms.

We thank the *Swiss National Science Foundation* for financial support, and Dr. *Orell* for a copy of the D2DNMR program.

Experimental Part

1. *General.* IR Spectra: *Perkin-Elmer 880* spectrophotometer equipped with a data station; 0.1 mm CaF_2 cells previously purged with N_2. ^{13}C-NMR Spectra: *Bruker WH 360* (90.55 MHz); δ in ppm relative to TMS, J(C,C) in Hz, samples enriched to *ca.* 30% ^{13}CO. 2D-^{13}C-NMR Spectra: COSY experiments, typically 256 t_1 increments with 2-K transients, spectral width 900.90 Hz in the F_2 domain and 450.45 Hz in the F_1 domain; NOESY experiments (mixing times indicated in the text), typically 512 increments with 2-K transients, spectral width 1190.0 Hz in the F_2 domain and 599.52 Hz in the F_1 domain; a squared sine bell was applied in both domains prior to *Fourier* transformation. Microanalyses were carried out by *Ilse Beetz*, Mikroanalytisches Laboratorium, Kronach, Germany.

2. *Monosubstituted Complexes.* Clusters **1**, **2**, **5**, and **7** were prepared by the literature methods indicated in the text.

Undecacarbonyl(thiocyanato)tetrairidium Tetraethylammonium ($NEt_4[Ir_4(CO)_{11}(SCN)]$, **3**). A soln. of **2** (200 mg, 0.15 mmol) in THF (80 ml) containing a suspension of AgSCN (75 mg, 0.45 mmol) was stirred for 12 h at r.t., then filtered through *Celite* to eliminate AgI and excess AgSCN. The orange soln. was evaporated and the product crystallised from CH_2Cl_2/Et_2O giving **3** (157 mg, 83%). IR (CH_2Cl_2, 298 K): 2108*w*, 2083*m*, 2049*s*, 2012*s*, 1841*m*, 1819*m* (CO). ^{13}C-NMR ($CD_2Cl_2/(D_8)$THF 1:1, 160 K): 213.7 (*s*, 2, *a*); 201.1 (*s*, 1, *b*); 175.7 (*s*, 1, *f*); 174.0 (*s*, 2, *d*); 157.1, 155.4 (2*s*, 2 each, *c* and *e*); 155.8 (*s*, 1, *g*). Anal. calc. for $C_{20}H_{20}Ir_4N_2O_{11}S$ (1265.33): C 18.99, H 1.59, N 2.21, S 2.53; found: C 19.09, H 1.65, N 2.24, S 2.42.

Undecacarbonyl(nitrito)tetrairidium Tetraethylammonium ($NEt_4[Ir_4(CO)_{11}(NO_2)]$, **4**). A soln. of **2** (200 mg, 0.15 mmol) in CH_2Cl_2 (80 ml) was stirred with $AgNO_2$ (74 mg, 0.225 mmol) for 2 h at r.t., then filtered through *Celite*. The yellow-orange solution was evaporated and the product crystallised from THF/Et_2O giving **4** (122 mg, 86%). IR (CH_2Cl_2, 298 K): 2085*m*, 2051*s*, 1826*m* (CO). IR (nujol): 2085*m*, 2052*s*, 2009*s*, 1829*m*, 1807*m* (CO); 1309*s*, 816*m* (NO_2). ^{13}C-NMR ($CD_2Cl_2/(D_8)$THF 1:1, 170 K): 214.9 (*s*, 2, *a*); 200.6 (*s*, 1, *b*); 176.0 (*s*, 1, *f*); 173.6 (*s*, 2, *d*); 158.3, 154.5 (2*s*, 2 each, *c* and *e*); 152.1 (*s*, 1, *g*). Anal. calc. for $C_{19}H_{20}Ir_4N_2O_{13}$ (1253.26): C 18.21, H 1.61, N 2.24; found: C 18.27, H 1.63, N 2.27.

Undecacarbonyl(triarylphosphine)tetrairidium Complexes **6–9**. A typical procedure is given for **9**. A soln. of **2** (400 mg, 0.30 mmol) and $P(4\text{-}(Me_2N)C_6M_4)_3$ (113.6 mg, 0.29 mmol) was stirred for 2 h at 273 K. The volume of the soln. was reduced to 40 ml at 1 mbar and 273 K, and MeOH was added. The yellow precipitate was crystallised from CH_2Cl_2/heptane giving **9** (350 mg, 79%). Other yields are: **6** (86%), **7** (93%), **8** (94%). IR (C_6H_{12}, 298 K): for **6**: 2090*s*, 2069*w*, 2055*vs*, 2036*s*, 2026*s*, 2018*s*, 2005*w*, 1890*vw*, 1856*s*, 1828*m* (CO); for **8**: 2085*s*, 2069*w*, 2052*vs*, 2033*m*, 2021*s*, 2013*s*, 1999*w*, 1888*vw*, 1855*s*, 1828*m*; for **9**: 2082*s*, 2070*w*, 2049*vs*, 2030*m*, 2018*s*, 2010*s*, 1974*vw*, 1886*vw*, 1851*s*, 1828*s*. IR in nujol also show three bands under 1900 cm^{-1}. $^{31}P\{^1H\}$-NMR (CD_2Cl_2, 213 K, 85% H_3PO_4 as external reference): for **6**: −15.42 (−10.9 for free $P(4\text{-}ClC_6H_4)_3$); for **7**: −12.07 (−7.94 for free PPh_3); for **8**: −16.32 (−13.04 for free $P(4\text{-}MeO)C_6H_4)_3$); for **9**: −16.82 (−14.40 for free $P(4\text{-}(Me_2N)C_6H_4)_3$). ^{13}C-NMR ($CD_2Cl_2$, 190 K; δ's are successively given for signals *a* (*s*, 2), *b* (*t*, 1), *f* (*d*, 1), *d* (*s*, 2), *c* and *e* (2*s*, 2 each), and *g* (*d*, 1)): for **6**: 204.2; 193.7 (J(C,C) = 8.5 from COSY spectrum); 170.6; 169.4; 157.1; 156.8; 155.5 (J(C,P) = 27 Hz); for **7**: 204.5; 194.5 (J(C,C) = 8); 171.2; 169.7; 157.5; 156.8; 155.5 (J(C,P) = 26); for **8**: 205.2; 194.8 (J(C,C) = 8.5); 169.8; 157.8; 156.9; 155.4 (J(C,P) = 25); for **9**: 205.9; 195.8; 172.9 (J(C,C) = 8); 170.2; 158.6; 157.2; 155.6 (J(C,P) = 24).

3. *Disubstituted Complexes.* The preparation of cluster **10** differs from the original one of *Stutz* and *Shapley* [4], who have also reported its ^{13}C-NMR spectrum. Clusters **11** and **12** were prepared by the literature method [16].

Decacarbonylbis(methyldiphenylphosphine)tetrairidium ($[Ir_4(CO)_{10}(PMePh_2)_2]$, **10**). A soln. of **1** (300 mg, 0.23 mmol) and $PMePh_2$ (78 mg, 0.39 mmol) in CH_2Cl_2 (50 ml) was stirred for 90 min at 273 K, then evaporated to dryness. The residue was washed with cold hexane (2 × 5 ml), extracted with CH_2Cl_2 (5 ml), and the extract was chromatographed on a plate of silica gel (*Merck 60F-254*, 20 × 20 × 0.2 cm) using CH_2Cl_2/hexane 1:4. Crystallisation from CH_2Cl_2/MeOH gave $[Ir_4(CO)_{11}(PMePh_2)]$ [4] (80 mg, 27%) and yellow crystals of **10** (185 mg, 55%). IR (C_6H_{12}, 298 K): 2066*vs*, 2040*vs*, 2010*s*, 2003*vs*, 1999 (sh), 1990 (sh), 2001*m*, 1870*w*, 1827*s*, 1798*s* (CO). $^{31}P\{^1H\}$-NMR ((D$_8$)toluene, 240 K, 85% H_3PO_4 as external reference): −28,8, −6.7. ^{13}C-NMR: see [4] and text.

Decacarbonylbis(η$_1$-diphenylphosphinobutane)tetrairidium ($[Ir_4(CO)_{10}(\eta_1\text{-dppb})_2]$. A soln. of $[Ir_4(CO)_{10}$(cycloocta-1,5-diene)] [11] (254 mg, 0.22 mmol) in CH_2Cl_2/C_6H_6 2:1 was added dropwise to a stirred soln. of dppb (0.66 g, 1.55 mmol) in CH_2Cl_2 (200 ml) at −20°, then gradually heated to r.t. for 4 h. After evaporation to dryness, the residue was taken up in cold C_6H_6 (15 ml) and chromatographed on a plate of silica gel using CH_2Cl_2/hexane 1:2. The major product was crystallised from CH_2Cl_2/MeOH giving yellow crystals of the title compound (0.118 mmol, 54%). IR (THF, 298 K): 2057*m*, 2032*s*, 1998*vs*, 1969*w*, 1956*w*, 1821*w*, 1801*w* (CO). $^1P\{^1H\}$-NMR (CD_2Cl_2, 200 K): 6.4, −17.3, −18.1, −18.3. ^{13}C-NMR (CD_2Cl_2, 200 K): 215.9, 206.6, 205.0, 174.4 (4*s*, 1 each); 172.4, 159.5 (2*d*, 1 each, J(C,P) = 14.4, and 25.0, resp.); 159.1, 158.7 (2*s*, 2 each); 157.3 (*d*, 1, J(C,P) = 6); 155.6 (*s*, 1). Anal. calc. for $C_{66}H_{56}Ir_4O_{10}P_4$: C 41.68, H 2.97; found: C 42.04, H 3.22.

Decacarbonylbis(diphenylphosphinopropane)tetrairidium ($[Ir_4(CO)_{10}(\mu_2\text{-dppp})]$, **11**) *and Decacarbonylbis(diphenylphosphinomethane)tetrairidium* ($[Ir_4(CO)_{10}(\mu_2\text{-dppm})]$, **12**). ^{31}P-NMR: see text and [16]. ^{13}C-NMR ((D$_8$)toluene, 240 K) of **11**: 222.1 (*s*, 1, *a*); 200.8 (*s*, 2, *b*); 174.6 (*s*, 2, *f*); 172.5 (*s*, 1, *d*); 164.7, 160.0 (2*s*, 1 each, *c* and *e*); 157.1 (*d*, 2 J(C,P) = 27.4, *g*). ^{13}C-NMR (CD_2Cl_2, 185 K) of **12**: 221.7 (*s*, 1 *a*); 205.6 (*s*, 2 *b*); 178.5 (*s*, 2 *f*); 171.4 (*s*, 1 *d*); 161.3 (2*s*, 1 each, *c* and *e*); 156.3 (*m*, 2, *g*).

Decacarbonylbis(diphenylarsinomethane)tetrairidium ($[Ir_4(CO)_{10}(\mu_2\text{-dpam})]$. A soln. of **2** (500 mg, 0.374 mmol) and dpam (177 mg, 0.374 mmol) in THF (150 ml) was stirred with $AgBF_4$ (73 mg, 0.374 mmol) for 2 h at 263 K under Ar. The suspension was reduced in volume, filtered, and chromatographed on a plate of silica gel with CH_2Cl_2/hexane 2:1. The first fraction was crystallised from CH_2Cl_2/heptane giving **13** (413 mg, 72%). The second fraction gave $[Ir_4(CO)_8(dpam)_2]$ (50 mg, 7%). IR (THF, 298 K): 2074*s*, 2042*s*, 2022*vs*, 2014*vs*, 1991*m*, 1972 (sh), 1865*w*, 1833*s*, 1797*s* (CO). ^{13}C-NMR: see text. Anal. calc. for $As_2C_{35}H_{22}Ir_4O_{10}$ (1521.19): C 27.63, H 1.45; found: C 27.56, H 1.35.

Decacarbonyl[μ$_2$-bis(methylthio)methane]tetrairidium ($[Ir_4(CO)_{10}(\mu_2\text{-}CH_3SCH_2SCH_3)]$, **14**). A soln. of **2** (272 mg, 0.204 mmol) and bis(methylthio)methane (259 μl, 2.54 mmol) in CH_2Cl_2 (130 ml) was stirred with $AgBF_4$ (51 mg, 0.26 mmol) for 1 h at 258 K under Ar, then passed through a column of silica gel at 258 K using CH_2Cl_2. The soln. was evaporated to dryness at 263 K, and the residue was dissolved in THF and heated in THF for 25 h at 333 K. Chromatography on a plate of silica gel using CH_2Cl_2/hexane 1:1 gave two fractions. Recrystallisation from CH_2Cl_2/heptane gave **14** (55%) and $[Ir_4(CO)_{11}(\eta_1\text{-}CH_3SCH_2SCH_3)]$ (18%). The latter compound can be obtained in 64% yield, if chromatography is not preceded by heating the residue in THF. IR (CH_2Cl_2, 298 K) of **14**: 2085*s*, 2045*vs*, 2024*vs*, 1990 (sh), 1963 (sh), 1864*vw*, 1829*w*, 1787*w*. IR (nujol): 2086*s*, 2081*s*, 2049*s*, 2033*vs*, 2027*vs*, 2012*vs*, 2006*vs*, 1999*s*, 1989*s*. ^{1}H-NMR (CD_2Cl_2, 168 K): 2.73 (*s*, 2 CH_3); 7.98, 3.98 (2*d*, 1 H each, ^2J(H,H) = 7.3, CH_2). ^{13}C-NMR: see text. Cross-peaks in a 2D-COSY spectrum at 170 K confirmed the pseudo-*trans*-positions of *b* and *d*, and of *c* and *e*. Anal. calc. for $C_{13}H_8Ir_4O_{10}S_2$ (1157.20): C 13.49, H 0.70; found: C 13.60, H 0.69.

REFERENCES

[1] G. Suardi, A. Strawczynski, R. Ros, R. Roulet, F. Grepioni, D. Braga, *Helv. Chim. Acta* **1990,** *73,* 154.
[2] B. E. Mann, C. M. Spencer, A. K. Smith, *J. Organomet. Chem.* **1983,** *244,* C 17.
[3] B. E. Mann, B. T. Pickup, A. K. Smith, *J. Chem. Soc., Dalton Trans.* **1989,** 889.
[4] G. F. Stutz, J. R. Shapley, *J. Am. Chem. Soc.* **1977,** *99,* 607.
[5] B. E. Mann, M. D. Vargas, R. Khadar, *J. Chem. Soc., Dalton Trans.* **1992,** 1725.
[6] A. Strawczynski, R. Ros, R. Roulet, *Helv. Chim. Acta* **1988,** *71,* 867.
[7] D. Braga, R. Ros, R. Roulet, *J. Organomet. Chem.* **1985,** *286,* C8.
[8] G. F. Stuntz, J. R. Shapley, *J. Organomet. Chem.* **1981,** *213,* 389.
[9] A. Orlandi, R. Ros, R. Roulet, *Helv. Chim. Acta* **1991,** *74,* 1464.
[10] M. R. Churchill, J. P. Hutchinson, *Inorg. Chem.* **1979,** *18,* 2451.
[11] A. Strawczynski, R. Ros, R. Roulet, F. Grepioni, D. Braga, *Helv. Chim. Acta* **1988,** *71,* 1885.
[12] P. Chini, G. Ciani, L. Garlaschelli, M. Manassero, S. Martinengo, A. Sironi, F. Canziani, *J. Organomet. Chem.* **1978,** *152,* C35; L. Garlaschelli, S. Martinengo, P. Chini, *ibid.* **1981,** *213,* 379.

[13] R. E. Stevens, P. C. C. Liu, W. L. Gladfelter, *J. Organomet. Chem.* **1985,** *287,* 133.
[14] G. F. Stuntz, J. R. Shapley, *Inorg. Chem.* **1976,** *15,* 1994.
[15] K. J. Karle, J. R. Norton, *J. Am. Chem. Soc.* **1974,** *96,* 6812.
[16] R. Ros, A. Scrivanti, V. G. Albano, D. Braga, L. Garlaschelli, *J. Chem. Soc., Dalton Trans.,* **1986,** 2411.
[17] R. Della Pergola, L. Garlaschelli, S. Martinengo, F. Demartin, M. Manassero, M. Sansoni, *Gazz. Chim. Ital.* **1987,** *117,* 245.
[18] M. P. Brown, D. Burns, M. M. Harding, S. Maggin, A. K. Smith, *Inorg. Chim. Acta* **1989,** *162,* 287.
[19] G. Ciani, M. Manassero, A. Sironi, *J. Organomet. Chem.* **1980,** *199,* 271.
[20] E. W. Abel, T. P. J. Coston, K. G. Orell, V. Sik, D. Stephenson, *J. Magn. Reson.* **1986,** *70,* 34.
[21] EXCHANGE, Program Library, Computing Center, University of Lausanne.
[22] C. A. Tolman, *Chem. Rev.* **1977,** *77,* 313; T. Bartik, T. Himmler, H.-G. Schulte, K. Seevogel, *J. Organomet. Chem.* **1984,** *272,* 29.
[23] A. Orlandi, U. Frey, G. Suardi, A. E. Merbach, R. Roulet, *Inorg. Chem.* **1992,** *31,* 1304.
[24] R. Giovanetti, Tesi di Laurea, Università di Padova, 1988.
[25] A. Strawczynski, R. Ros, R. Roulet, D. Braga, C. Gradella, F. Grepioni, *Inorg. Chim. Acta* **1990,** *170,* 17.
[26] F. H. Carre, F. A. Cotton, B. A. Frenz, *Inorg. Chem.* **1976,** *15,* 380.
[27] M. M. Harding, B. S. Nicholls, A. K. Smith, *Acta Crystallogr., Sect. C* **1980,** *40,* 790.
[28] C. S. Johnson Jr., C. G. Moreland, *J. Chem. Educ.* **1973,** *50,* 477.
[29] D. Braga, F. Grepioni, *J. Organomet. Chem.* **1987,** *336,* C9.